ORIGINAL ARTICLE

QTL and eQTL mapping associated with host response to *Candidatus* Liberibacter asiaticus in citrandarins

Tatiany Aparecida Teixeira Soratto[1,2] · Maiara Curtolo[1,3] · Samanta Marengo[4] · Ana Lúcia Dezotti[1] ·
Rômulo Pedro Macêdo Lima[1,5] · Rodrigo Gazaffi[6] · Marcos Antonio Machado[1] · Mariângela Cristofani-Yaly[1]

Abstract

Huanglongbing (HLB) is a severe disease of citrus caused by the bacterium *Candidatus* Liberibacter. In America, the most common species is *Candidatus* Liberibacter asiaticus (CLas). In a previous study of the Citrus-HLB pathosystem, our group found differences in CLas multiplication in a population of hybrids obtained by hybridization between *Citrus sunki* Hort. Ex Tan. and *Poncirus trifoliata* (L.) Raf. cv. Rubidoux. The bacterial concentration was higher in *C. sunki* than in *P. trifoliata*. Thus, this study aims to map phenotypic (QTL) and gene expression (eQTL) data associated with host response to CLas in the linkage groups (LGs) of the previously constructed parental maps of *C. sunki* and *P. trifoliata* cv. Rubidoux. For the phenotypic analysis, we used a population of 79 F1 hybrids (termed citrandarins) between *C. sunki* and *P. trifoliata*. CLas and starch were quantified in the leaves of the plants two years after pathogen inoculation, allowing the classification of hybrids as resistant, tolerant, and susceptible. The expression of 14 candidate genes was measured in 72 hybrids of the population and used as expression data for the eQTL mapping. We located nine QTL and 52 eQTL in the *C. sunki* map and 17 QTL and 40 eQTL in the *P. trifoliata* map. The overlap of eQTL of the majority of genes with QTL from the phenotypic data indicates that the genes are related to the phenotype and are probably related to pathogen infection.

Keywords Huanglongbing · Phenotypic analysis · Gene expression · Citrandarins

Introduction

Huanglongbing (HLB) is currently considered the most devastating disease of citrus crops (Morgan et al. 2014; Raiol-Junior et al. 2017). The severity of the disease is indicated by the appearance of symptoms that lead to premature fruit drop and the absence of fruits in branches that present symptoms. Monitoring for the presence of psyllids, spraying with insecticides, inspecting plants, and eradicating those with symptoms are still the main methods used to control the disease and typically incur costs equivalent to 5 to 10% of the production (Fan et al. 2013; Fundecitrus 2017).

There is no cure for HLB, and its symptoms are responsible for severe losses in production and fruit quality. Dissemination of the disease can occur by bacterial transmission from infected plants to healthy plants through psyllid insect vectors (*Diaphorina citri* or *Trioza eritraea*) and by the propagation of infected citrus tissues (Bové 2006). A one-year-old orchard in which 1% of the plants infected with HLB will have a total production reduction of 26.5% in the eighth year. These data confirm the difficulty in controlling the disease and the importance of its eradication (Fundecitrus 2017).

Of the 16 Liberibacter species described, only three fastidious α-Proteobacteria species are associated with HLB in citrus; these are *Candidatus* Liberibacter asiaticus (CLas), *Candidatus* Liberibacter americanus, and *Candidatus*

✉ Mariângela Cristofani-Yaly
   mariangela@ccsm.br

[1] Centro APTA Citros Sylvio Moreira, Instituto Agronômico de Campinas, 13490-970 Cordeirópolis, SP, Brazil

[2] Laboratório de Bioinformática, Centro de Ciências Biológicas, Universidade Federal de Santa Catarina, 88040-970 Florianópolis, SC, Brazil

[3] Universidade Estadual de Campinas, 13083-862 Campinas, SP, Brazil

[4] Hill Laboratories, 3204 Hamilton, New Zealand

[5] Departamento de Genética, Instituto de Biociências, Universidade do Estado de São Paulo, 18618-000 Botucatu, SP, Brazil

[6] Centro de Ciências Agrárias, Universidade Federal de São Carlos, 13600-970 Araras, SP, Brazil

Liberibacter africanus (Wang et al. 2017). The simplest way to identify CLas infection is a visual inspection of the plants for symptoms; other, more accurate techniques include serologic assays, electron microscopy, biological assays, DNA probes, loop-mediated isothermal amplification, PCR, and real-time quantitative PCR (qPCR) (Rigano et al. 2014). Real-time PCR has become the most commonly used method due to its reliability, identification sensitivity, detection, and usefulness in bacterial quantification (Li et al. 2006; Rigano et al. 2014). Equally important, starch quantification has also become routine in the analysis of CLas-infected plants, since several studies have reported that starch accumulation is higher in HLB-positive plants than in HLB-negative plants (Kim et al. 2009; Fan et al. 2010; Koh et al. 2012; Aritua et al. 2013; Boava et al. 2017).

Yellow shoots, blotchy mottled leaves, upright, hardened and small leaves, leaves showing zinc deficiency and corky veins, twig dieback, stunted growth, and tree decline are characteristic symptoms of HLB. These symptoms are considered a consequence of the cellular, physiological, and molecular changes that occur in the plant in response to infection (Boava et al. 2017; Wang et al. 2017). Although no specific mechanism through which CLas exerts its pathogenicity has been conclusively identified, the symptoms appears related to be phloem dysfunction (Machado et al. 2010; Koh et al. 2012). The pathogenic mechanism through which the bacteria act is associated with the induction of metabolic disturbances in the host, probably in response to bacterial products, leading to an imbalance in carbohydrate metabolism. Symptomatic leaves have been shown to accumulate excessive amounts of starch. The retention of starch and sucrose in infected citrus leaves suggests loss of transport capacity for photoassimilates (Dalio et al. 2017).

The deposition of high amounts of callose and phloem proteins (PP2) on the phloem sieve plates interferes with the transport of photoassimilates from their sources in leaves to the sink organs (Koh et al. 2012; Boava et al. 2017; Wang et al. 2017), resulting in excessive starch accumulation in leaf chloroplasts (Wang and Trivedi 2013; Boava et al. 2017). Starch accumulation causes the disintegration of the chloroplast thylakoid system, producing the yellowing leaf mottle symptom (Etxeberria et al. 2009). CLas has grave consequences for the host plant, producing nutritional deficiencies and affecting plant growth, fruit ripening, and seed development (Kim et al. 2009).

A possible source of tolerance/resistance to HLB is *P. trifoliata*. Studies have shown that the trifoliate group has a higher tolerance of HLB than other citrus groups (Folimonova et al. 2009; Boscariol-Camargo et al. 2010; Albrecht and Bowman 2012; Boava et al. 2017, Huang et al. 2018). This species does not present any symptoms or starch accumulation during bacterial multiplication; starch accumulation remains low or almost non-existent (Boava et al. 2017).

Hybrids called citrandarins, resulted from controlled crosses between *C. sunki* (a susceptible phenotype) and *P. trifoliata*, show high variability in CLas titer and starch content. According to Boava et al. (2017), the susceptible group was HLB-positive and showed a significant difference in starch accumulation, while the tolerant group was HLB-positive with no significant difference in starch accumulation, and the resistant group, was diagnosed as HLB-negative, and presented no changes in starch levels.

A strategy that can be used to investigate the response mechanisms of the citrus - HLB pathology system is gene expression data mapping using expression quantitative trait loci (eQTL). eQTL are gene regions identified based on the abundance of specific gene transcripts. The integrated analysis of genotypic and quantitative transcription data may help in the identification of genes involved in specific phenotypes (Wang et al. 2014). Jansen and Nap (2001) proposed genomic genetics as a technique in which mapping of quantitative loci and gene expression analysis is used to identify the association between the allelic status of a genome region and the levels of gene transcripts. In citrus, a few eQTL mapping studies have been conducted, including studies of carotenoid metabolism (Sugiyama et al. 2014) and resistance to *Phytophthora nicotianae* Breda de Haan (*Phytophthora parasitica* Dastur) in a population of *C. sunki* and *P. trifoliata* hybrids (Lima et al. 2018).

The present work aimed to identify QTL involved in the citrus - HLB pathosystem interaction using CLas and starch quantification and to identify eQTL using the gene expression values in the linkage groups (LGs) of previously constructed maps of *P. trifoliata* and *C. sunki* (Curtolo et al. 2018). CLas quantification and starch accumulation in hybrids of *C. sunki* and *P. trifoliata*, as well as the expression of candidate genes analysis related to CLas multiplication by qPCR in the parents and hybrids, were employed in the experiments.

Materials and methods

Plant material and experimental design

The experiment was conducted in a greenhouse at the Centro de Citricultura Sylvio Moreira of the Instituto Agronômico (IAC), Cordeirópolis/SP, in 2013. The plants used in the experiment are part of an F_1 hybrids population obtained from a cross between *C. sunki* Hort. Ex Tan. and *P. trifoliata* (L.) Raf. cv. Rubidoux; *C. sunki* was used in controlled hybridization as the female parent (HLB-susceptible), and *P. trifoliata*, which is considered HLB tolerant, was used as the male pollen donor.

The experimental block consisted of genotypes of *C. sunki*, *P. trifoliata*, and 79 hybrids that were multiplied by bud grafting into Rangpur lime (*C. limonia* Osb.). After six months, the plants were inoculated with two buds from

HLB-infected plants; the buds were grafted on opposite sides of the plant's primary stem. These infected buds were collected from HLB-symptomatic branches of Pera sweet orange (*C. sinensis* L. Osb.).

The plants were arranged in a completely randomized experimental design, with six biological replicates of each genotype (three plants inoculated with infected buds (Inoculated) and three plants inoculated with healthy buds (Control)). We collected leaves and petioles 24 months after CLas inoculation for bacteria and starch quantification. Leaves were also placed in liquid nitrogen and stored at -80 °C until RNA extraction for gene expression.

DNA extraction

Leaves of the same age and position were collected from all four sides of the plant. Eight-leaf petioles were combined, and 200 mg of leaves were ground in the presence of two beads (3 mm diameter) in 2 ml microtubes at 30 Hz for 120 s using a TissueLyser II (Qiagen). DNA extraction was performed using the CTAB method (Murray and Thompson 1980). The precipitated DNA was dissolved in 50 µL of DNAse-free water. The quality of the DNA was verified by electrophoresis on 1% agarose gels. DNA concentrations were determined using a NanoDrop™ 8000 spectrophotometer (Thermo Scientific) and adjusted to 100 ng/µL.

CLas quantification by qPCR

The amplifications were performed in duplicate (Table 1) in 14 µL reactions containing 6.25 µL of 1X TaqMan Universal Master Mix (Applied Biosystem), 216 nM each primer and 135 nM each probe (HLBp) in a thermocycler (ABI Prism 7500 Sequence Detection System, Applied Biosystems) (Li et al. 2006). GAPDH was used as an endogenous gene with 270 nM each primer and 135 nM each probe (Boava et al. 2015). The reaction volume was brought to 11 µL with water, and 3 µL of DNA was added. Each 96-well PCR plate included two wells with water as negative PCR controls and two wells with CLas samples as positive controls. The PCR cycle conditions were 95 ºC for 5 min followed by 40 cycles of 95

ºC for 30 s and 58 ºC for 45 s. Optimization of reagent concentrations, including primers and probes, was performed using known HLB-positive and HLB-negative DNAs.

A standard curve was used to calculate the bacterial titer. The target fragment of CLas was amplified using the 16S ribosomal DNA (rDNA) of the bacterium as described by Li et al. (2006). The expected target fragment was separated by low-melting 2% agarose gel electrophoresis, isolated *in situ* and purified using a Qiaquick gel extraction kit (Qiagen) according to the manufacturer's instructions. The DNA was eluted and used for ligation with the pGEM®-T vector (Promega). The recombinant plasmid was used to transform competent *E. coli* DH5α cells. The recombinant plasmid was extracted using the Pure Yield™ Plasmid Miniprep System (Promega) according to the manufacturer's instructions, sequenced and aligned using BLASTN. The plasmid standard solution was quantified on a NanoDrop™ 8000 spectrophotometer (Thermo Scientific) and serially diluted 10-fold from the original 10^{-10} target DNA solution; the dilutions were used to generate a curve (dsDNA = 6.6×10^5 g mol^{-1} kb^{-1}) according to Wang et al. (2006). The number of copies [CN] of 16S rDNA per µL was based on the equation CN = (M x N) / (L x D), where M = minimum nucleic acid concentration detected (g mL^{-1}), N = Avogadro's number (6.022×10^{23}), L = nucleic acid length in kpb (total length of insertion plasmid), and D = conversion factor from 1 kb of nucleic acid to daltons Wang et al. (2006).

Starch quantification

For starch quantification, the enzymatic method was applied to 10 mg of dry leaves according to Amaral et al. (2007). To remove sugars, pigments, phenols, and other soluble substances, four extractions were performed, each in 500 µL of 80% ethanol at 80 °C for 20 min, yielding 2 mL of ethanolic extract. The precipitate was dried overnight at room temperature. Then, 0.5 mL (120 U mL^{-1}) of *Bacillus licheniformis* thermostable α-amylase (EC 3.3.1.1; Megazyme) diluted in 10 mM MOPS buffer (pH 6.5) was added, and the mixture was incubated at 75 °C for 30 min; this was repeated once. The samples were then cooled to 50 °C, 0.5 ml of a solution containing 30 U mL^{-1} of *Aspergillus niger* amyloglucosidase

Table 1 Primer sequences for CLas quantification

Gene	Primer name	Sequence 5'- 3'	References
16S rDNA	HLBas (Forward)	TCGAGCGCGTATGCAATACG	Li et al. (2006)
	HLBr (Reverse)	CTACCTTTTTCTACGGGATAACGC	
	HLBp (TaqMan probe)	AGACGGGTGAGTAACGCG	
Glyceraldehyde-3-phosphate dehydrogenase	GAPDH-f (Forward)	GGTCAGTGGAAGCACAACGA	Fan et al. (2010)
	GAPDH-r (Reverse)	GAGTACTAAAATGTACCTGAATCCGAAA	
	GAPDH-p (TaqMan probe)	TCCTCTTCGGTGAGAAGCCAGTCGCT	

(EC 3.2.1.3; Megazyme) diluted in 100 mM sodium acetate buffer (pH 4.5) was added, the mixture was incubated at 50 °C for 30 min, and the glucosidase treatment was repeated once. After the incubations, 100 µL of 0.8 M perchloric acid was added to stop the reaction and precipitate proteins. The samples were then centrifuged (2 min at 10,000 g), and the glucose released in the hydrolysis process was quantified. A mixture of 20 µL of extract and 300 µL of Liquiform PAP Glucose Reagent (CENTERLAB) containing glucose oxidase ($\sim$ 11,000 U mL^{-1}), peroxidase ($\sim$ 700 U mL^{-1}), 290 µmol L^{-1} of 4-aminoantipyrine, and 50 mM phenol (pH 7.5), was incubated for 15 min at 37 °C, and the absorbance of the sample at a wavelength of 490 nm was then determined using a spectrophotometer. A glucose solution (SIGMA) at concentrations of 0, 2.5, 5.0, 7.5 and 10 µg/mL was used to construct a standard curve.

Phenotypic data analysis

The Ct value was considered as a continuous variable varying from 1 to 34. Assuming that Ct value is inversely proportional to the amount of bacteria, lower Ct values would indicate less tolerant genotypes. The sample was considered positive when Ct value was below 34 (Boava et al. 2015). If the genotype replicates showed a discrepancy in results, we considered only the positive replicates.

Two parameters were considered for CLas quantification: the Ct values (qPCR result) and the CLas 16S fragment copy number, which was obtained from the standard curve of the HLB primers using log (base 10) transformed data. For the starch quantification, two groups were considered: individuals without CLas inoculation (Control) and individuals with CLas inoculation (Inoculated).

The statistical model used in the analysis was $y = Xr + Zg + \epsilon$, where y = data vector, r = replicate effects vector (assumed to be fixed) added to the overall mean, g = vector of the individual genotypic effects (considered as random), and ϵ = errors or residuals vector (random). Uppercase characters represent the incidence of matrices for the outcome mentioned above. Analyses were performed using R software (www.r-project.org), and the values of the genotypic prediction (BLUPs - *Best Linear Unbiased Prediction*) were estimated. The heritability of each trait was measured based on the variance and the coefficient of variation obtained in the phenotypic analysis.

The genetic correlations between the traits were obtained by determining Spearman's correlation coefficients for the individual genotypic values. These correlations were tested assuming a global significance level of 0.01. The analyses were performed using R statistical software.

RNA extraction and cDNA synthesis

Total RNA was extracted with lithium chloride (LiCl) according to the protocol described by Chang et al. (1993) and adapted by Porto et al. (2010). The extractions were performed in 72 hybrids, *P. trifoliata* and *C. sunki*, using three inoculated biological replicates and three mock-inoculated biological replicates of each genotype two years after inoculation. Traces of genomic DNA were eliminated using RNAse-free DNase I (Fermentas Life Sciences). Furthermore, purification with phenol-chloroform and precipitation of RNA with ethanol were performed to remove proteins and free nucleotides.

The quality of the RNA was verified by electrophoresis after separation on a formaldehyde agarose gel (denaturant), and its concentration was determined using a NanoDrop ND-8000 spectrophotometer (Thermo Scientific). The cDNAs were synthesized from 1.0 µg of total RNA using Superscript III (200 U/mL) (Invitrogen) with an oligo (dT) primer (dT12-18, Invitrogen) according to the manufacturer's instructions. Subsequently, the cDNA was diluted 1:25 in RNAse-free water. The three biological replicates of cDNA (25 µL each) were mixed to form a gene pool of samples in a single tube containing 75 µL of diluted cDNA from each genotype; this DNA was used in the gene expression and eQTL mapping assays.

qPCR for gene expression

For gene expression analyses, we used 72 hybrids of the population as well as the parent species. The RT-qPCR analysis evaluated the expression of 14 genes involved in sugar and carbohydrate metabolism, starch transport and degradation, and phloem functionality. The FBOX and GAPC2 genes were used as endogenous controls (Table 2). Our group obtained some genes involved in sugar and carbohydrate metabolism from a previous RNA-seq study (data not shown). This study was based on differential expression of transcripts in a comparison of plants infected with CLas and control plants of *P. trifoliata*, *C. sunki*, and their hybrids. Starch degradation genes were established based on the work presented by Fan et al. (2010); these are the main genes involved in the transient degradation pathway of starch in leaves. The genes involved in phloem functionality were based on the transcriptome study of susceptible citrus genotypes conducted by Mafra et al. (2013).

The primers flanking the gene regions were synthesized using Primer Express 2.0 software (Applied Biosystems) and checked for specificity using the Primer-BLAST tool in the NCBI (National Center for Biotechnology Information) database. The synthesized primers were validated by standard PCR. Then, qPCR amplifications for the gene expression analysis were performed using 7.5 µL of GoTaq qPCR Master Mix (Promega), 3 µL of cDNA (1:25 dilution) taken from the gene

Table 2 Sequences of primers used in qPCR for gene expression analysis

Gene code	Gene	Function	ID[1]	Forward/Reverse 5' - 3'	Source
UDP	UDP-glucose	Transferase activity, transferring hexosyl groups, metabolic process	Cs2g23750	CGCTTGGAACACAAAAGGAATAAA/ AATTGAATTGGAGCTTGATGGA	Own design
T6PP	Trehalose-6-phosphate synthase	Catalytic activity, trehalose biosynthetic process, metabolic process	Cs3g09800	TTTGCATAGTCCATTTCCTTCA/ AAAGCCAATCAAGTCCGAAT	Own design
CARBOX	Carboxylesterase-Related	Hydrolase activity, metabolic process	Cs9g06500	ACAAGAAGCGTTTGGAATATTTGA/ AACTCGGCTTACCTGAACCA	Own design
PAE	Pectin Acetylesterase	Hydrolase activity, cell wall organization	Cs3g10420	TTCACTTCAGAGGAGCAAGG/ AGCGGAACAACCAGTAAGTA	Own design
GLUC	Beta-glucosidase	Catalytic activity, hydrolase activity, carbohydrate metabolic process	Cs6g17840	CGACTGCCCAAATTCACAAA/ GATGTTACTTCCTCTGCATAATCT	Own design
GALAC	Beta-galactosidase	Catalytic activity, hydrolase activity, carbohydrate metabolic process	Cs4g14090	GTTCATTCACAATGTCTGGGTT/ TTCACTTGGGTCAATCTTAACA	Own design
BAM3	Beta-amylase	Polysaccharide catabolic process, catalytic activity, carbohydrate metabolic process	Cs5g07550	CCATGGGTGCTTGAAGAAAT/ GTTC TTCCTCTGAGCAACGG	(Fan et al. 2010)
MEX1	Maltose exporter	Maltose transport	Cs7g15380	CATGTGGATGCCAGTTTCAC/ CGTGGGATCAGAAGTCCATT	(Fan et al. 2010)
BAC2	Mitochondrial arginine transporter BAC2	Mitochondrial carrier protein, transmembrane transport	Cs1g14950	ACAAGATCCAAACAAGCAGAT/ ACAGTGATACTAAGTCCTCGATAT	Own design
NRAMP	Metal Transporter Nramp	Natural resistance-associated macrophage protein, metal ion transporter, metal ion (Mn2+/Fe2+)	Cs3g19960	TTTCACTTCTTGGTGCTATGGTTA/ TCCTTGATGCTCCTAACAGAT	Own design
EREB	Ethylene responsive element binding protein	Sequence-specific DNA binding transcription factor activity, regulation of transcription	Cs9g10650	GACTAATAGCAGAAGCCACACC/ TTTCCTCTGTTGTTGAACTCACC	Own design
NAC2	NAC domain protein NAC2	DNA binding, regulation of transcription, DNA-dependent	Cs3g19890	CGCCGAAATCGATCTTTACA/ TTTGGATACTTCCGATCCCTA	Own design
PP2B15	Phloem-protein B15	Protein binding	Cs3g14740	AGATTAGTGTTGCCGCTGGT/ GAAGGAAGGGTTTCCAGGTC	(Mafra et al. 2013)
PP2B10	Phloem-protein B10	Protein binding	Cs6g02680	AGATTAGTGTTGCCGCTGGT/ GAAGGAAGGGTTTCCAGGTC	(Mafra et al. 2013)
FBOX	F-box family protein	Endogenous control		GGCTGAGAGGTTCGAGTGTT/ GGCTGTTTGCATGACTGAAGA	(Mafra et al. 2012)
GAPC2	Glyceraldehyde-3-phosphate dehydrogenase C2	Endogenous control		TCTTGCCTGCTTTGAATGGA/ TGTGA GGTCAACCACTGCGACAT	(Mafra et al. 2012)

[1] Identification of the genes obtained in the database is available at http://citrus.hzau.edu.cn/cgi-bin/orange/search

pool formed by the three biological replicates of that genotype, 200 nM of each primer and water to a final volume of 15 μL. The 7500 Fast Real-Time PCR System (Applied Biosystems) was used with the following conditions: 50 °C for 2 min, 95 °C for 10 min, and 40 cycles of 95 °C for 15 s and 60 °C for 1 min. For each reaction, a dissociation curve was obtained to assess possible nonspecific contamination and to verify the reactions; only reactions in which a single peak appeared in the curve were used in the analysis. In addition, the reactions were performed in duplicate using controls without cDNA to detect possible contamination. All plates were pipetted using Eppendorf's automated epMotion system to eliminate manual pipetting errors and to maximize the reproducibility of the assays.

Normalization of qPCR data and gene expression analyses

The expression stability for each reference gene was assessed using GenEx v.6 software (De Spiegelaere et al. 2015). Two treatments were considered in the study: plants inoculated with CLas (infected group) and mock-inoculated (control group). Relative amounts, expression levels, fold change values and the stability of expression of endogenous genes were determined according to Lima et al. (2018).

The amplification efficiency and Ct data were calculated for each qPCR reaction using Real-time PCR Miner software (Zhao and Fernald 2005). For each gene, the average efficiency of all the PCR reactions was calculated. The mean Ct values of the two technical replicates of each genotype analyzed were also determined. Relative quantification was performed using the $2^{-\Delta\Delta CT}$ method for each different set of qPCR conditions and used as a parameter in the calculation of the expression levels of each sample (Livak and Schmittgen 2001).

The expression levels of each genotype were calculated using the geometric mean of the relative quantities estimated for the two reference genes as a normalization factor. The calculation of expression level was performed by taking the ratio between the value of the relative expression of the target gene and the normalization factor for the genotype under analysis for each sample. Finally, the Foldchange values of inoculated individuals relative to mock-inoculated ones were calculated as the ratio of the expression levels of the infected group and the control group.

Gene expression data analyses

Four qPCR plates were used for each analyzed gene. Half of the plate was used for 18 of the genotypes and two parents from the infected group, while the other half of the plate was used for the other 18 genotypes and two parents from the control group. The mixed linear model was used, using the "nlme" package of the R program (www.r-project.org) to perform the comparison among the four plates for a gene.

The parents and the plate were considered fixed variables, and the genotypes were considered random variables. Thus, genotypic and residual variances and BLUPs for the means of adjusted expressions were obtained. The heritability for each trait was estimated based on the variance and the coefficient of variation determined in the gene expression analysis.

To obtain a gene expression profile comparing the expression of the 14 candidate genes among the 72 hybrids and the two parents, *C. sunki* and *P. trifoliata*, Log2 Foldchange values were used as input to the MeV (MultiExperiment Viewer) program v. 4.9 (http://sourceforge.net/projects/mev-tm4/) using hierarchical clustering (HCL) and the Pearson correlation as metric distance; the results were visualized as a heatmap.

QTL and eQTL mapping

The pre-built linkage maps of *C. sunki* and *P. trifoliata* (Curtolo et al. 2018) were used in QTL and eQTL mapping. Both maps were constructed using DArT-seq™ molecular markers in OneMap Software (Margarido et al. 2007). The grouping was performed used the likelihood ratio, considering a LOD score = 8 and the maximum recombination fraction of 0.3. We used the means of the phenotypic data (starch quantification and Ct values) in the segregating population of 72 hybrids for QTL mapping. In order to detect QTL involved in starch accumulation, both data from mock-inoculated and inoculated plants were included in the analysis. While for CLas QTL mapping only the Ct values from inoculated plants were considered. Fold change values of the relative expression in the segregating population adjusted by the mixed model were used as inputs for the eQTL mapping.

The data were analyzed through composite interval mapping (CIM) (Zeng 1993), using the FullsibQTL package of the R program (Gazaffi et al. 2014). Cofactors were included in the model to control the QTL and eQTL located outside the mapping. A maximum of 20 cofactors was used to avoid over-parameterization of the model. The limit values for evidencing (LOD score) QTL and eQTL were obtained using a significance level of 0.05 and 1,000 permutations (Churchill and Doerge 1994) according to the modification proposed by Chen and Storey (2006). The phenotypic variations (R^2) explained by QTL and eQTL were also estimated.

Results

CLas and starch quantification

Two characteristics, the Ct values and the log of the 16S copy number, were taken into account in performing CLas quantification in the samples. The starch quantification was evaluated in two groups: mock-inoculated individuals (Control plants) and inoculated individuals. The results of starch quantification were presented as mg glucose/g dry weight. Based

Table 3 Components of variance, heritability and adjusted means for bacterial quantification (Ct values and log of 16S copies number) and starch quantification (mock-inoculated and inoculated plants)

Characteristics		Mean	Vg	Ve	Vp	h² (%)	CVg (%)	CVr (%)
Quant. CLas	Ct	25.36	23.77	14.56	38.33	62.01	19.22	15.05
	log	5.0428	2.157	1.771	3.93	54.91	29.12	26.39
Quant. Starch	Non-inoc.	18.03	5.84	30.85	36.69	15.91	13.40	30.81
	Inoc.	46.92	829.50	159.70	989.20	83.86	61.38	26.93

Vg = genotypic variance; Ve = environmental variance; Vp = phenotypic variance; h^2 = heritability coefficient; CVr = coefficient of variation of the residue; CVg = coefficient of variation for genotypic variance

on these results, it was possible to estimate the genetic parameters (heritability, variances, and coefficients of variation) for the measured variables (bacterial and starch quantification) two years after inoculation (Table 3)

In the inoculated group, high values of heritability (h^2) were observed both for starch concentration (approximately 84%) and for CLas quantification (62% for Ct and 55% for log). The starch and bacteria quantification presented significant Spearman correlations for all analyzed variables ranging from 0.44 to 0.48 (p < 0.01).

Figure 1 shows the mean´s distribution for the CLas (Ct values) and starch (inoculated group) quantification. For both characteristics, one can verify transgressive segregation, once there are hybrids with upper and lower means comparing to the parents. It should be noted that the histograms showed a continuous distribution varying from 21.20 to 34.95, with average of 25.36 and median 23.73. This provided a slight positive skewed distribution. The same pattern also happened for starch (inoculated group). Considering the parents, *P. trifoliata* showed a lower starch quantification and a higher Ct value, while *C. sunki* had a higher starch concentration and lower Ct value.

Figure 2 shows the hybrids plotted for the CLas (Ct values) and starch (inoculated group) quantification. Based on this analysis, the 79 hybrids were classified into three groups taking into account their CLas and starch concentrations after

CLas inoculation. The resistant group (R) presents high Ct values that are inversely proportional to the number of bacteria in the plant. The samples of hybrids with Ct values higher than 32 were considerate resistant (group R). The tolerant group (T) comprised the plants with CLas, but they are starch-free or contain only low concentrations of starch compared to inoculated and mock-inoculated plants, as well *P. trifoliata* (reported as tolerant to the pathogen). The hybrids with less than 50 mg glucose / g dry weight of starch were considered as tolerant (group T). The susceptible group (S) was composed of the hybrids with high CLas and starch quantification, and the *C. sunki* (reported previously as susceptible). Individuals 149 and 279 were not grouped.

Gene expression

High values of heritability (h^2) ranging from 0.50 to 0.99 were observed (Table 4). Most genes, with the exception of NRAMP (h^2 = 50.01%), EREB (h^2 = 68.63%), and PP2B15 (h^2 = 64.83%), showed high heritability values (h^2 > 90%).

A heatmap was constructed using hierarchical clustering (HCL) of the log2Foldchange values of 14 target genes in the 74 selected genotypes (72 hybrids and parents) (Fig. 3). Using Pearson's correlation as the metric distance, the best possible intra- and intervariable groupings with similar gene expression profiles were obtained. The Log2Foldchange data ranged from

Fig. 1 Histograms of means for the CLas (Ct values) and starch (inoculated group) quantification. On the right starch quantification data in the inoculated group (mg glucose / g dry weight); on the left, CLas quantification (Ct values) are shown. The female parent (*C. sunki*) is shown in red, and the male parent (*P. trifoliata*) is shown in green
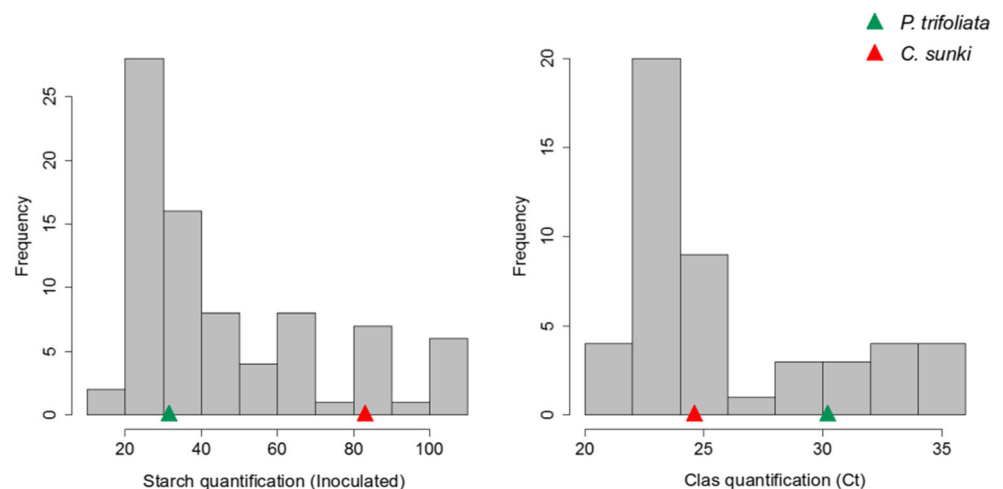
Fig. 2 Phenotypic data scatter plot. The starch quantification data in the inoculated group is presented in mg glucose / g dry weight on the y-axis. On the x-axis, the CLas quantification presented in Ct values. Colored by the group resistant (R), susceptible (S), and Tolerant (T) determined using the threshold of 32 Ct and 50 mg glucose / g dry weight. The parentals are highlighted with red arrows. The hybrids H149 and H279 were not grouped
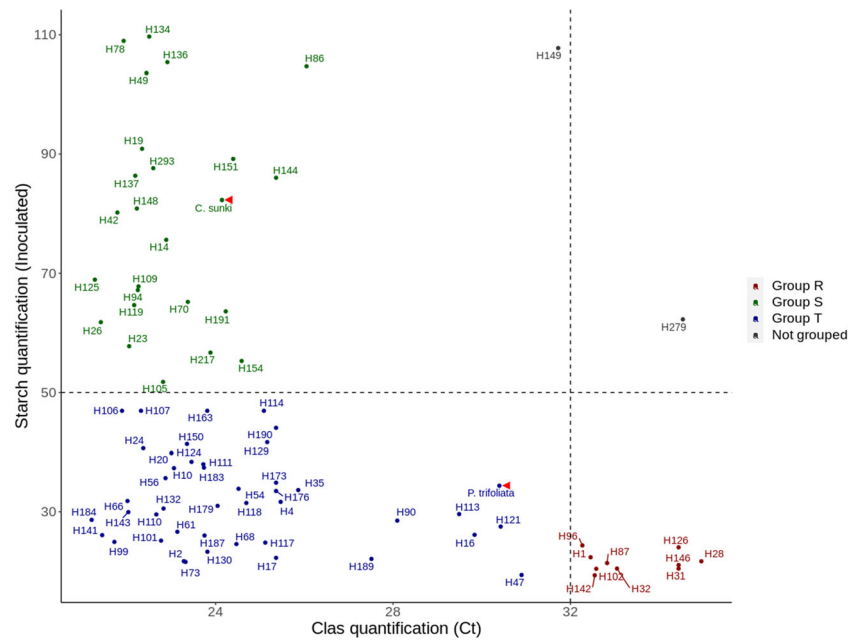
−6.27 to 7.39. The genotypes were divided into four secondary clusters distributed in two main clusters, while the genes in the four secondary clusters were arranged in three main clusters.

QTL mapping

Using the genetic maps previously constructed for each parent of the hybrid progeny (Curtolo et al. 2018) and phenotypic data from Ct values and starch quantification, QTL associated with CLas and starch quantification in the citrus - HLB pathosystem were detected.

In the *P. trifoliata* map, eight QTL were found for CLas multiplication (Ct values), three were found for starch concentration in the control group, and six were found in the inoculated group (Table 5; Fig. 4). In the *C. sunki* map, four QTL were found for starch concentration in the control group, two were found in the inoculated group, and three were found based on the Ct values (Table 6; Fig. 5).

For starch quantification, the QTL detected in the control group (non inoculated) were related to different genotypes of the progeny, and they were not related to CLas infection. They are different from the QTL obtained from the analysis of the inoculated group. The difference can be justified based on the greater variability in starch levels in hybrids infected with CLas.

The consistent QTL had LOD scores above the critical LOD score calculated using the permutation test for each mapped trait. For the *P. trifoliata* map, the critical LOD score ranged from 2.44 to 2.60, while for the *C. sunki* map, it ranged from 2.66 to 2.99. The confidence interval for determination of the presence of QTL was 95%. In the *P. trifoliata* map, the QTL LOD score ranged from 2.70 to 11.16. The phenotypic variation (R^2) explained by the markers ranged from 1.19–15.69% (Table 5). In the *C. sunki* map, the LOD score ranged from 3.54 to 11.18, and the R^2 values ranged from 0.46–11.62% (Table 6).

Eight QTL for CLas quantification (Ct values), located in LGs: 1 (56.11 cM), 2 (120.08 cM), 4 (257.93 cM), 6 (160.72 cM), 7 (137.28 cM), 8 (2.92 cM), 9 (39.58 cM), and 10 (215.88 cM), were found in the *P. trifoliata* map. They explained 55.01% of the observed phenotypic variation. For the starch quantification, three QTL were found using the data of

Table 4 Estimates of genotypic and phenotypic variances, heritability and coefficients of variation for gene expression

Genes	Vg	Vf	h² (%)	CVr (%)	CVg (%)
UDP	0.93	0.96	96.62	17.08	91.36
T6PP	1.64	1.69	97.32	14.87	89.60
CARBOX	1.69	1.70	99.46	7.36	99.66
PAE	6.41	6.47	99.04	17.08	173.52
GLUC	0.66	0.71	93.77	21.08	81.77
GALAC	1.20	1.22	98.23	9.90	73.86
BAM3	4.34	4.41	98.41	9.41	73.94
MEX1	0.88	0.91	96.19	16.66	83.66
BAC2	1.97	1.98	99.07	7.65	79.12
NRAMP	4.79	9.57	50.01	131.39	131.41
EREB	1.41	2.06	68.63	45.93	67.93
NAC2	2.77	2.78	99.66	5.63	95.71
PP2B15	1101.50	1699.00	64.83	180.26	244.76
PP2B10	1.10	1.13	97.56	16.64	105.23

Vg = genotypic variance; Vf = phenotypic variance; h2 = heritability; CVr = coefficient of variation of the residue; CVg = coefficient of variation for genotypic variance

Fig. 3 Heatmap of the gene expression profile by clustering analysis between 14 evaluated target genes with 74 selected genotypes (72 hybrids with the parents: *P. trifoliata* and *C. sunki*). The heatmap using Log$_2$Foldchange values in the MeV (MultiExperiment Viewer) program v. 4.9. Names of genes and gene hierarchical cluster are shown in the top of the figure. Log2Fold change expression values representation ranges from yellow (highest expression) to blue (lowest expression). Sample names (74 selected genotypes) are shown on the right side of the figure, and the sample hierarchical cluster is shown on the left side
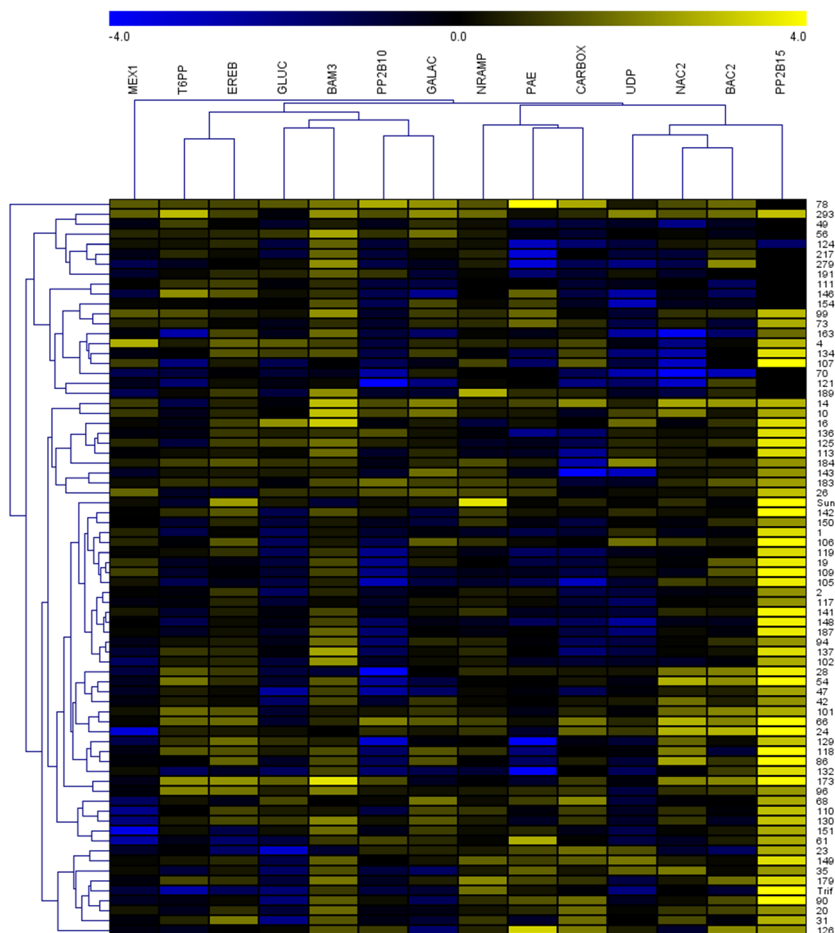
the control group in LGs 2 (267.25 cM), 6 (28.95 cM), and 7 (177.00 cM), explaining a total of 11.38% of the phenotypic variation. Using the data of the inoculated group, six QTL were detected in LGs 1 (122.00 cM), 2 (149.59 cM), 3 (85.61 cM), 5 (381.53), 6 (209.35 cM), and 10 (95.30 cM),

with R^2 of 41.49% when analyzed together (Table 5). In LG 2 and LG 6, there were overlaps of QTL for CLas multiplication (Ct values) and starch quantification.

In the *C. sunki* map, three QTL were found for CLas quantification (Ct values); these were located in LGs 5 (412.07

Table 5 QTL identified from the starch quantification in the control group (Cont.), inoculated group (Inoc.) and the CLas quantification (Ct values) in *Poncirus trifoliata* map

Character	Flanking Markers	LG	cM	LOD score	p	R^2 (%)
Starch (Cont.)	100046231|F|0	2	267.25	4.54	-0.29	2.92
Starch (Cont.)	100041038|F|0	6	28.95	5.80	0.25	1.63
Starch (Cont.)	100063185|F|0-100033220|F|0	7	177.00	4.93	-0.23	6.83
Starch (Inoc.)	100032204|F|0-100035034|F|0	1	122.00	5.09	2.12	1.19
Starch (Inoc.)	100043207|F|0	2	149.59	8.94	-10.82	8.34
Starch (Inoc.)	100068766|F|0	3	85.61	5.78	9.92	10.30
Starch (Inoc.)	100066277|F|0	5	381.53	3.25	7.25	2.93
Starch (Inoc.)	100043581|F|0	6	209.35	11.16	-12.82	15.69
Starch (Inoc.)	100048556|F|0	10	95.30	2.70	6.28	3.04
CLas (Ct)	100036184|F|0	1	56.11	3.61	-0.92	1.25
CLas (Ct)	100079987|F|0	2	120.08	4.78	1.31	10.39
CLas (Ct)	100034430|F|0	4	257.93	4.13	-1.20	6.77
CLas (Ct)	100043664|F|0	6	160.72	5.00	-1.06	1.73
CLas (Ct)	100048658|F|0	7	137.28	7.12	1.41	7.60
CLas (Ct)	100125184|F|0	8	2.92	8.71	1.79	13.41
CLas (Ct)	100035369|F|0	9	39.58	4.47	-1.15	4.31
CLas (Ct)	100034525|F|0	10	215.88	8.27	-1.50	9.55

LG = linkage group, cM = start position in centiMorgans of identified QTL, p = effect of QTL on *P. trifoliata* parent, R^2 = phenotypic variation explained by QTL in percentage (%)
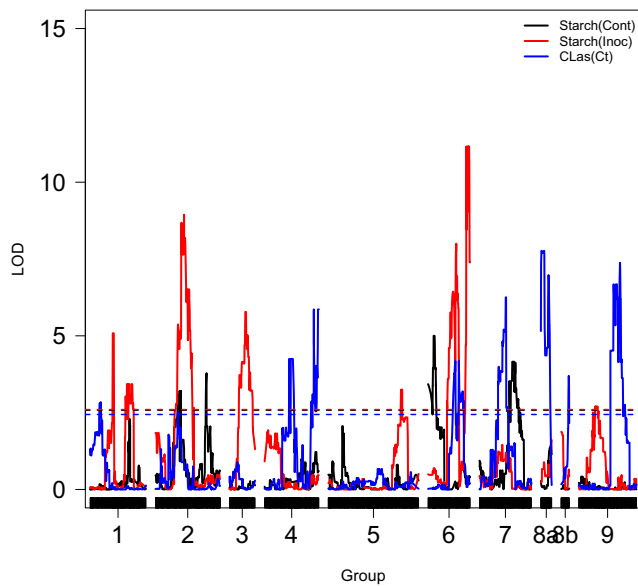
Fig. 4 Detection of QTL related to CLas and starch quantification in the *Poncirus trifoliata* linkage map. QTL associated with CLas quantification (Ct values) are shown in blue. QTL associated with starch quantification are shown in red for the inoculated group and in black for the control group. Y-axis: LOD values; X-axis: distance in centiMorgans. The horizontal lines are the critical LOD scores defined by the permutation test with significance of 5%

cM), 6 (13.48 cM), and 7 (105.12 cM) and together explained 23.45% of the phenotypic variation. For the starch quantification, four QTL were found in LGs 5 (323.29 cM), 6 (171.36 cM), 7 (171.44 cM), and 8 (34.00 cM) in the control group, explaining a total of 23.69% of the phenotypic variation. In the inoculated group, two QTL were detected in LGs 3 (127.39 cM) and 4 (0.84 cM), with a total R^2 of 14.91% (Table 6).

eQTL mapping

A total of 92 eQTL were detected, comprising 40 for the *P. trifoliata* map, with approximately three eQTL per gene,

and 52 for the *C. sunki* map, with approximately four eQTL per gene. Only the NRAMP gene in the *P. trifoliata* map and the PAE gene in the *C. sunki* map did not present eQTL (Figs. 6 and 7).

Tables 7 and 8 present the results of eQTL mapping for the two parental maps. For the eQTL found on the *P. trifoliata* map, the critical LOD score ranged from 2.65 to 4.35, while the LOD scores for the detected eQTL ranged from 3.01 to 17.61, with the amount of variation in the phenotype (R^2) explained by the eQTL ranging from 0.01–18.85% (Table 7; Fig. 6). For the *C. sunki* map, the critical LOD score ranged from 2.35 to 4.82, while the LOD scores varied from 2.55 to 16.65, showing consistent regions, with R^2 values varying from 0.25–25.41% (Table 8; Fig. 7).

In the present study, a total of eleven hotspots were identified in the *P. trifoliata* map, and twelve were identified in the *C. sunki* map, representing approximately one hotspot per LG for both maps (Table 9). We have identified overlaps between eQTL and QTL (Table 10). In the *P. trifoliata* map, two overlaps were observed between QTL related to starch quantification in LGs 1 and 5 and eQTL, and four overlaps were observed between QTL related to CLas quantification (Ct values) in LGs 4, 7, 8b and 9 and eQTL. In the *C. sunki* map, three overlaps of QTL related to CLas quantification with eQTL were found in LGs 5, 6, and 7; only one QTL related to starch quantification in LG 3 overlapped with eQTL.

Discussion

Estimates of the genetic variance among the progeny individuals were higher than the environmental variances for the characteristics under study. The observed high heritability and genotypic variability indicate that selection for resistance in the progeny can be

Table 6 QTL identified through starch quantification in the control group (Cont.), inoculated group (Inoc.) and CLas quantification (Ct values) in the *Citrus sunki* map

Character	Flanking markers	LG	cM	LOD *score*	q	R^2 (%)
Starch (Cont.)	100033230|F|0	5	323.29	6.79	-0.28	4.44
Starch (Cont.)	100173875|F|0	6	171.36	6.51	0.25	0.46
Starch (Cont.)	100009568|F|0	7	171.44	9.16	0.52	11.62
Starch (Cont.)	100197417|F|0	8	34.00	11.18	0.37	7.17
Starch (Inoc.)	100014756|F|0	3	127.39	3.54	-8.22	5.06
Starch (Inoc.)	100009269|F|0	4	0.84	3.88	-8.50	9.85
CLas (Ct)	100019677|F|0	5	412.07	4.65	1.21	7.97
CLas (Ct)	100047667|F|0	6	13.48	5.06	0.98	5.39
CLas (Ct)	100010739|F|0	7	105.12	8.73	-1.72	10.09

LG = linkage group, cM = start position in centiMorgans of identified QTL, p = effect of QTL on *Citrus sunki* parent, R^2 = phenotypic variation explained by QTL in percentage (%)
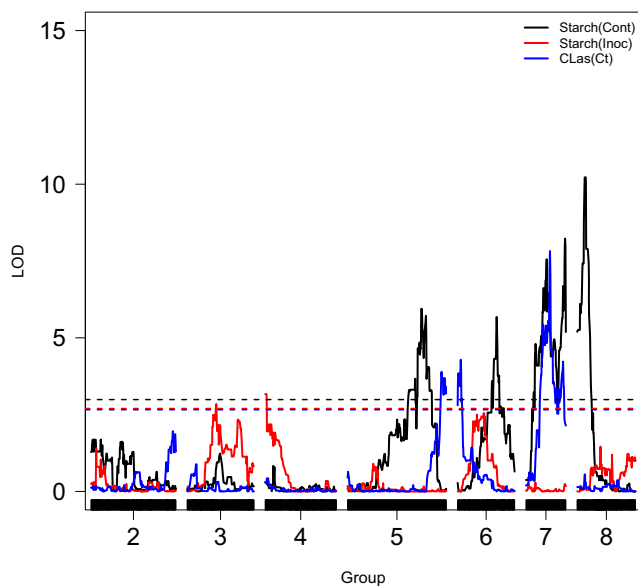
Fig. 5 Detection of QTL related with CLas and starch quantification in the *Citrus sunki* linkage map. In blue, QTL associated with CLas quantification (Ct values). In red, QTL associated with starch quantification in the inoculated group, and in black in the control group. Y-axis: LOD values; X-axis: distance in centiMorgans. The horizontal lines are the critical LOD scores defined by the permutation test with significance of 5%

successfully performed; in other words, the hybrids present adequate genetic variability for selection. These results indicate that a large portion of the phenotypic variation in both starch concentration and CLas level observed is due to genetic factors. For starch levels, a low h^2 value, 15.91, was found in the mock-inoculated samples, indicating that in the absence of disease the genotypic variability in starch accumulation is low.

The CLas titer was higher in *C. sunki* than in *P. trifoliata*. Considerable variation in the CLas titer was observed among the 79 different hybrids (Fig. 1). The results are consistent with those of other studies in which it was shown that *P. trifoliata* and some hybrids are tolerant/resistant to CLas infection (Folimonova et al. 2009; Boscariol-Camargo et al. 2010; Albrecht and Bowman 2012; Boava et al. 2015; 2017, Huang et al. 2018). This also indicates that genetic factors of the *P. trifoliata* parent may play a role in the different responses to CLas infection observed among the progeny genotype in the present work.

Boava et al. (2017) conducted a study of 13 hybrids of the same population used in the present study 18 months after bacterial inoculation and classified them into three similar groups with respect to bacterial and starch quantification. Two years after CLas inoculation, hybrid H31 was resistant, confirming the findings of the previous work, while two other hybrids (H90 and H118) that were resistant 18 months after inoculation became tolerant. Hybrids H35 and H66 remained tolerant, while H102 was classified in the present work as

resistant, being previously identified as tolerant in Boava et al. (2017). This can be explained in two possible ways: either the plant is responding to the pathogen or the bacterium has not been detected due to its irregular distribution in the plant (Teixeira et al. 2008).

Boava et al. (2015) previously studied these hybrids under field conditions and observed differences in CLas multiplication in both parents and progeny. However, the evidence obtained in that study could not be used to distinguish whether the response of *P. trifoliata* and the hybrids was related to the CLas infection or to a non-preference of psyllids for *P. trifoliata*; some studies have shown that psyllids have low preference for *P. trifoliata* (Richardson and Hall 2014; Hall et al. 2015).

The high levels of starch found in the leaves of the infected plants suggest that phloem function in the susceptible genotypes was affected by the CLas infection, confirming data obtained by other authors (Kim et al. 2009; Etxeberria et al. 2009; Fan et al. 2010; Koh et al. 2012; Aritua et al. 2013; Boava et al. 2015; Boava et al. 2017).

Considering the gene expression results, the high values of h^2 indicate that the expression levels of almost all of the genes evaluated in the progeny were related to the CLas infection response. Characteristics with greater genetic control have higher heritability values than those that are highly influenced by the environment (Lynch and Walsh 1998; Visscher et al. 2008).

In the cluster analysis shown in the first heatmap (Fig. 3), the genes PP2B15, EREB, and BAM3 were predominantly upregulated in the study population. Therefore, these genes may contribute more strongly than other genes to resistance to CLas infection. On the other hand, the genes PP2B10, UDP, and GLUC were predominantly downregulated, indicating that they did not contribute to the defense response of the different phenotypes to CLas infection. Taking into account the genotypes, *P. trifoliata* formed a group with hybrids H20, H35, H90 and H179, which are considered tolerant, as well as with hybrids 31 and 126, which are considered resistant. These hybrids are promising materials for study of the basis of resistance to CLas and can be used in future research related to HLB disease. Some hybrids considered susceptible (H19, H94, H105, H109, H119, H137, and H148) were in the same group as the *C. sunki* parent.

Regarding the genes (Fig. 3), the MEX1 gene formed a single group. It is involved in starch degradation and it is also relevant to maltose transport (Ferro et al. 2003). According to Fan et al. (2010), the abundance of MEX1 transcripts is lower in infected leaves than in uninfected leaves. Equally important, with the reduction in maltose levels, it is suggested that the impairment in starch degradation may contribute to the accumulation of starch in the infected leaves. The EREB and T6PP genes were grouped; the former encodes an enzyme that is putatively involved in trehalose biosynthesis (Aryal et al. 2017), and the latter encodes a transcription factor associated

Fig. 6 Distribution of eQTL in the *Poncirus trifoliata* map related to expression of 14 target genes. Y-axis: LOD values; X-axis: distance in centiMorgans. The horizontal lines with different colors are the critical LOD scores for each target gene defined by the permutation test with significance of 5%
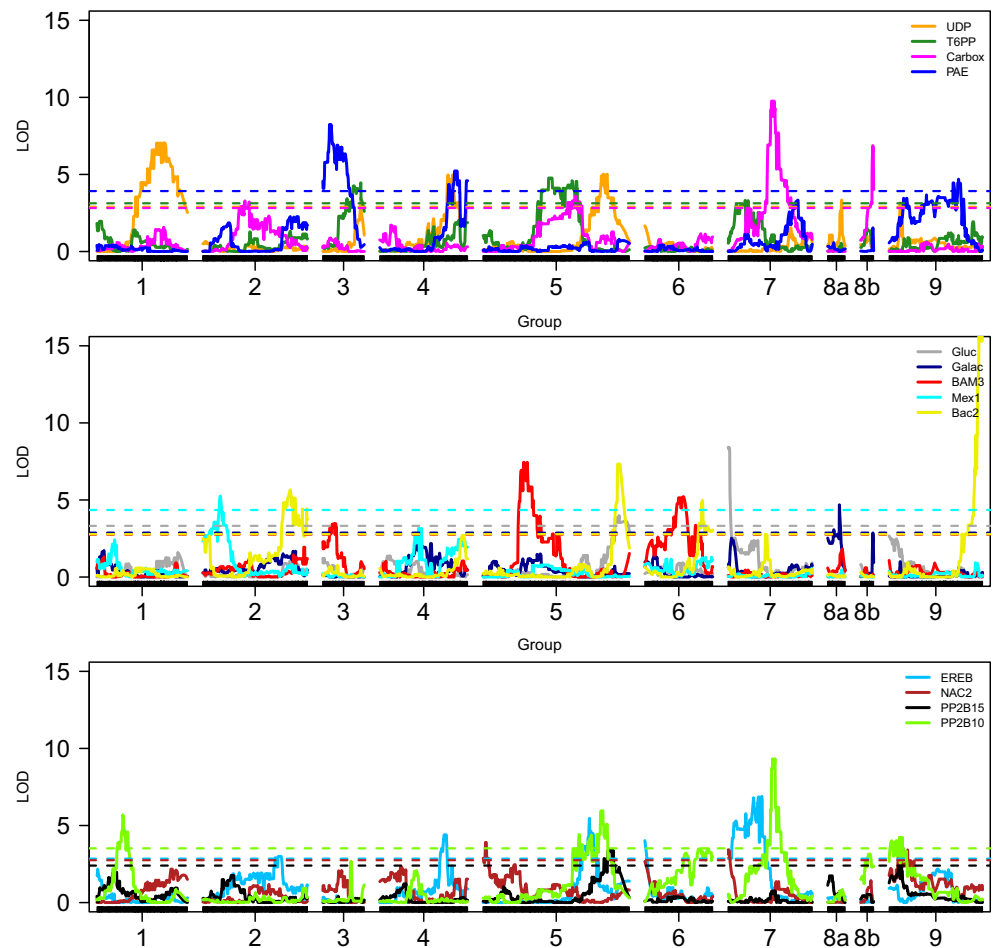

with the ethylene response (Asamizu et al. 2008). The GALAC, BAM3, GLUC, and PP2B10 genes formed another group. The first three of these are related to the metabolism of carbohydrates (Ishikawa et al. 2007; Gantulga et al. 2008; Zhang et al. 2011), while the latter is involved with phloem functionality (Mafra et al. 2013).

The CARBOX, PAE, and NRAMP genes also were grouped; the former is involved in hydrolase activity (McLennan 2006). The PAE gene plays a role in controlling the mechanical properties of the cell wall (Philippe et al. 2017). It may contribute to the control of plant-pathogen interactions in response to a variety of biotic stresses, including penetration of the plant by biotrophic fungi and necrotrophs, and thereby play a significant role in plant defense (Philippe et al. 2017). The NRAMP gene is related to metal ion transport (Cellier et al. 1995). The last group was formed by the genes UDP, NAC2, BAC2 and PP2B15. The UDP gene is related to glucose metabolic processes (Burchell et al. 1991). NAC2 (Ernst et al. 2004), BAC2 (Saurin et al. 1999), and PP2B15 (Mafra et al. 2013) are transcription factors for transmembrane transport, and PP2B15 is involved in phloem functionality (Mafra et al. 2013).

In a study of differentially expressed genes in trees infected by CLas (Wang et al. 2016), it was observed that 686 genes were differentially expressed (DE) between HLB-tolerant and HLB-susceptible citrus trees. Among these genes, only the genes encoding UDP-glucosyl transferase and beta-glucosidase were included among our studied genes. In our study, UDP-glucosyl transferase and beta-glucosidase were upregulated, and they were more highly expressed in the susceptible genotype.

QTL mapping procedure used in this study was presented in Gazaffi et al. (2014) and it was applied in Curtolo et al. (2018). This model was a powerful approach for QTL mapping allowing composite interval mapping based on different segregation patterns modeled by mixture models under normality. In our knowledge, QTL mapping developed in a non-normality assumption is not available for this scenario. Figure 1 may indicates CLas quantification and starch content as a non-normality traits. The skewed pattern may also indicate a mixture of two normal distributions, which is desirable for the used QTL mapping approach. This can be clearly illustrated with an eye inspection in CLas quantification histogram where two peaks are visible, a major one at Ct 22 and 24 and another one above Ct 30. Some other drawbacks could be

Fig. 7 Distribution of eQTL in the *Citrus sunki* map related to expression of 14 target genes. Y-axis: LOD values; X-axis: distance in centiMorgans. The horizontal lines with different colors are the critical LOD scores for each target gene defined by the permutation test with significance of 5%
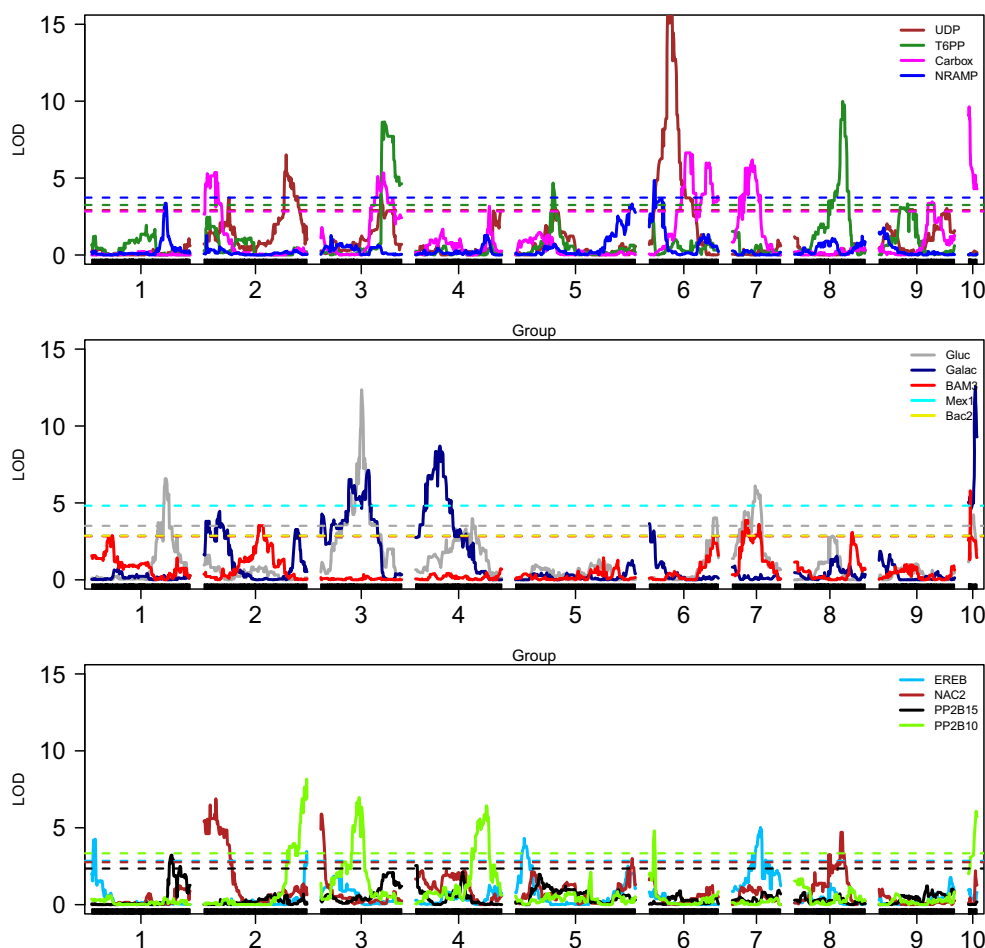
also stressed, such as bias during hypothesis test. For QTL mapping this was reduced by using permutation test, once threshold by an empirical distribution obtained by this dataset. Li et al. (2006) have developed a QTL mapping method based on inbred lines for dealing with ordinal traits. This model provides similar results then and standard QTL mapping methodology when more than five categories were observed. Earlier, Rebai (1997) has compared two approaches for non-normality trait. First the non-parametric approach which tend to perform in a similar way for data with exponential or others continuous distribution especially when sample size increases. The major disadvantage was the loss of QTL effect. The second one was the logistic regression for categorical traits which was slight superior than regression interval mapping but this difference reduces as the sample size increases and the distribution is symmetric. The sample size used in this work is consistent with the literature (Lima et al. 2018), especially dealing with a perennial crop. Considering the aspects present by Rebaï (1997) and Li et al. (2006), we chose to assume normality as a starting point for revealing information about related traits to HBL disease, once results are not frequent in literature. In this context, probably

moderate and lower QTLs would not be detected, but the mapped QTL can provide insights for further gene discovery studies.

Regarding the QTL mapping (Figs. 4 and 5), most of the QTL detected in the *C. sunki* and *P. trifoliata* maps had small effects, and a few had moderate R^2 values. QTL with small effect are generally identified in polygenic inheritance studies; they are responsible for less than 10% of the phenotypic variation (Anderson et al. 2007; Marengo, 2009), while QTL with moderate effects are those with R^2 values ranging from 10–30% (Asins et al. 2004). QTL with great effects are responsible for more than 45% of the observed phenotypic variation (Budahn et al. 2009). According to Anderson et al. (2007), many QTL mapping studies detect few loci with moderate R^2 values, while several other loci with small effects are found, similar to the findings of the present study. Lima et al. (2018) mapped QTL associated with resistance to *P. parasitica*, the causative agent of citrus gummosis, in the same population of citrandarins and also found few loci with moderate R^2 values and many with small effects.

Differences in the number of QTL detected were observed when comparing this work with the first report on

Table 7 eQTL identified from the expression values for each target gene in the *Poncirus trifoliata* map

Gene	LG	Flanking markers	cM	LOD score	q	R² (%)
UDP	1	100035177|F|0	203.34	7.03	-0.45	16.48
UDP	3	100093859|F|0	122.92	3.57	-0.34	5.11
UDP	4	100053681|F|0	235.24	5.01	-0.38	7.89
UDP	5	100021313|F|0	389.57	5.03	0.32	5.91
UDP	8a	100050766|F|0	45.31	3.35	0.29	4.91
UDP	9	100038391|F|0	35.97	3.19	0.30	2.32
T6PP	3	100020866|F|0	122.19	4.50	0.35	6.15
T6PP	5	100031383|F|0	221.64	4.77	0.33	4.76
T6PP	7	100028454|F|0	55.31	3.33	0.27	1.90
CARBOX	2	100036881|F|0-100027763|F|0	136.00	3.30	-0.23	0.02
CARBOX	5	100044221|F|0	298.14	3.60	-0.52	18.85
CARBOX	7	100015910|F|0	142.39	9.77	0.44	0.08
CARBOX	8b	100035369|F|0	39.58	6.87	0.44	4.74
PAE	3	100057532|F|0	26.36	8.25	-0.55	2.81
PAE	4	100161318|F|0-100051462|F|0	243.00	5.25	-0.41	2.08
PAE	9	100058156|F|0	224.34	4.69	0.40	1.78
GLUC	5	100089610|F|0	439.67	3.99	0.18	5.49
GLUC	7	100049762|F|0	1.11	8.43	0.38	18.16
GALAC	8a	100056835|F|0	37.63	4.69	-0.35	4.06
BAM3	3	100029311|F|0-100036111|F|0	37.00	3.47	-0.42	0.10
BAM3	5	100046237|F|0	142.38	7.45	-0.64	0.19
BAM3	6	100076894|F|0-100039672|F|0	124.00	5.23	0.45	2.94
MEX1	2	100051584|F|0	56.37	5.25	-0.24	0.10
BAC2	2	100178691|F|0	282.10	5.66	0.53	8.36
BAC2	5	100033599|F|0	440.40	7.34	0.50	6.71
BAC2	6	100084313|F|0	186.33	4.98	-0.34	6.06
BAC2	9	100069113|F|0	301.90	17.61	0.74	12.59
EREB	2	100026276|F|0-100042757|F|0	250.00	3.01	0.19	1.36
EREB	4	100025526|F|0	213.62	4.40	-0.26	2.19
EREB	5	100045322|F|0	343.47	5.48	0.29	4.65
EREB	6	100032182|F|0	0.00	4.04	-0.29	1.55
EREB	7	100057022|F|0	108.45	6.91	0.39	5.76
NAC2	5	100183597|F|0	9.38	3.90	0.36	3.11
NAC2	7	100196998|F|0	1.11	3.44	-0.45	5.58
NAC2	9	100061705|F|0	43.66	3.59	-0.38	5.75
PP2B15	5	100080169|F|0	405.31	3.55	2.76	1.02
PP2B10	1	100056564|F|0	83.90	5.70	-0.31	7.36
PP2B10	5	100068714|F|0	385.75	5.96	-0.30	3.30
PP2B10	7	100044511|F|0	151.17	9.33	-0.31	4.62
PP2B10	9	100043903|F|0	42.56	4.25	0.20	2.16

LG = linkage group, cM = start position in centiMorgans of identified QTL, p = effect of eQTL on *P. trifoliata* parent, R² = phenotypic variation explained by QTL in percentage (%)

identification of QTL related to HLB disease and tolerance (Huang et al. 2018), however both reports showed many regions associated with HLB tolerance, revealing citrus tolerance to HLB is likely polygenic. As reported by Huang et al. (2018), QTL for foliar symptoms were identified both in tolerant and susceptible parental maps, indicating that sweet orange can also show genetic factors in order to improve HLB tolerance. Nevertheless, some divergences in QTL results were observed between the two works, probably because the phenotypic analysis followed different methodologies. In

Table 8 eQTL identified from the expression values for each target gene in the *Citrus sunki* map

Gene	LG	Flanking markers	cM	LOD *score*	q	R^2 (%)
UDP	2	100016633|F|0	296.76	6.54	-0.37	10.72
UDP	3	100021476|F|0-100048216|F|0	217.00	3.91	-0.24	3.79
UDP	6	100197254|F|0	79.37	16.65	-0.59	20.34
UDP	9	100010814|F|0	244.35	3.04	0.23	3.71
T6PP	3	100011342|F|0	230.51	8.65	0.42	7.91
T6PP	5	100029469|F|0	135.55	4.69	-0.27	6.45
T6PP	8	100019860|F|0-100126693|F|0	174.00	10.01	0.39	5.09
T6PP	9	100063546|F|0	103.59	3.33	0.19	0.25
CARBOX	2	100005257|F|0	40.62	5.38	-0.43	6.92
CARBOX	3	100013218|F|0	227.02	5.34	-0.42	5.70
CARBOX	4	100005540|F|0	266.50	3.17	0.29	3.42
CARBOX	6	100034742|F|0-100046449|F|0	146.00	6.65	0.52	5.13
CARBOX	7	100026011|F|0	72.83	6.19	-0.43	9.38
CARBOX	9	100035814|F|0	191.91	3.47	-0.32	5.10
CARBOX	10	100201189|F|0-100137691|F|0	3.00	9.67	0.61	20.31
GLUC	1	100043790|F|0	266.68	6.58	0.21	5.41
GLUC	3	100043261|F|0	147.27	12.36	0.33	11.31
GLUC	4	100037909|F|0	205.99	3.98	-0.20	4.22
GLUC	6	100036283|F|0	243.14	4.03	0.17	7.52
GLUC	7	100013734|F|0	82.56	6.11	-0.19	7.63
GLUC	10	100202826|F|0	18.28	4.23	0.23	6.44
GALAC	2	100037187|F|0	56.77	4.46	-0.37	6.69
GALAC	3	100053032|F|0	172.53	7.12	0.57	13.10
GALAC	4	100031971|F|0-100043688|F|0	88.00	8.70	-0.47	5.32
GALAC	6	100181892|F|0	0.00	3.66	-0.27	4.61
GALAC	10	100171869|F|0	25.47	12.58	0.71	25.41
BAM3	1	100058307|F|0-100061132|F|0	74.00	2.90	-0.40	1.10
BAM3	2	100028862|F|0	206.52	3.53	-0.40	1.12
BAM3	7	100012855|F|0	49.01	3.88	-0.77	10.89
BAM3	8	100047420|F|0	208.85	3.12	0.53	3.43
BAM3	10	100156188|F|0	6.58	5.86	0.96	8.03
MEX1	6	100047667|F|0	13.48	10.11	-0.26	5.81
MEX1	9	100048503|F|0	160.22	4.85	0.17	2.32
BAC2	2	100022861|F|0	6.80	8.64	-0.45	8.00
BAC2	3	100026361|F|0	17.54	3.79	-0.30	2.65
BAC2	7	100040736|F|0	8.51	3.16	-0.24	2.04
NRAMP	6	100030612|F|0	18.09	4.85	-0.20	4.84
EREB	1	100186532|F|0	13.02	4.26	-0.28	9.19
EREB	2	100201571|F|0	370.59	3.46	-0.25	7.18
EREB	5	100188422|F|0	31.33	4.33	-0.26	6.77
EREB	7	100055682|F|0	102.13	5.02	-0.26	7.80
NAC2	2	100028817|F|0	42.76	6.89	-0.44	7.13
NAC2	3	100002208|F|0-100027934|F|0	2.00	6.00	-0.54	3.90
NAC2	5	100048739|F|0	420.98	3.01	-0.41	3.19
NAC2	8	100029816|F|0	170.12	4.71	0.37	2.89
PP2B15	1	100072566|F|0	288.66	3.22	-2.34	1.10
PP2B15	4	100063037|F|0	3.42	2.55	-3.53	1.43
PP2B10	2	100201571|F|0	370.59	8.17	0.36	6.17
PP2B10	3	100040067|F|0	138.01	6.99	0.37	4.84
PP2B10	4	100050457|F|0	257.33	6.44	-0.33	3.95
PP2B10	6	100030612|F|0	18.09	4.81	-0.38	13.66
PP2B10	10	100163575|F|0-100163311|F|0	28.00	6.09	0.32	7.43

LG = linkage group, cM = start position in centiMorgans of identified QTL, p = effect of eQTL on *Citrus sunki* parent, R^2 = phenotypic variation explained by eQTL in percentage (%)

present word, the phenotypic data for QTL analysis was based on CLas quantification and starch accumulation caused by inoculation by CLas in a greenhouse. In Huang et al. (2018), the phenotypic data for QTL analysis was based the evaluation of HLB symptoms assessed on a 6-point scale of foliar symptom and canopy damage in field trial carried out by visual evaluation.

The high heritability values ($h^2 > 60\%$) found both for starch accumulation in the inoculated group and CLas quantification (Ct values) are consistent with the detection of several QTL associated with CLas multiplication in the present study, mainly in the map of the tolerant parent *P. trifoliata*. The location of QTL and the magnitude of their genetic effects

Table 9 Relationship of genes that presented overlapping and localized eQTL in hotspots for each linkage group (LG) in the two genetic maps constructed for each parent

LG	*C. sunki* map	*P. trifoliata* map
1	GLUC and PP2B15	-
2	CARBOX, GALAC, BAC2 and NAC2 UDP, EREB and PP2B10	BAC2 and EREB
3	UDP, T6PP and CARBOX GLUC, GALAC and PP2B10 BAC2 and NAC2	UDP and T6PP PAE and BAM3
4	CARBOX, GLUC and PP2B10	UDP, PAE and EREB
5	-	UDP, GLUC, EREB, PP2B15 and PP2B10 T6PP and CARBOX
6	GALAC, MEX1, NRAMP and PP2B10	BAM3 and BAC2
7	CARBOX, GLUC, BAM3 and EREB	CARBOX and PP2B10 GLUC and NAC2
8	T6PP and NAC2	UDP and GALAC
9	CARBOX and MEX1	NAC2 and PP2B10
10	CARBOX, GLUC, GALAC, BAM3 and PP2B10	-

contribute to the detection and selection of possible loci responsible for the variation in evaluated phenotypic characteristics (Grattapaglia 2004).

According to Shi et al. (2007), eQTL may have high detection power even in small and medium-sized populations. Furthermore, since the methodology established by the software for QTL mapping is similar to that for eQTL mapping, a population size greater than 50 is sufficient to provide high resolution in mapping and detecting QTL/eQTL with small effects. The larger the population size, the saturation of the genetic linkage map and the heritability of the phenotypic character, the greater is the genomic information related to the mapping (Young 1994; Yan et al. 2009).

Eleven genes (UDP, T6PP, CARBOX, PAE, GLUC, GALAC, BAM3, MEX1, BAC2, NAC2, and PP2B10) with heritability values greater than 90% (Table 4) were found in the present work. Except for the PAE gene, all of these genes presented at least one eQTL related to CLas infection; genes such as

UDP, CARBOX, and PP2B10 were present in the genetic maps of both parents (Figs. 6 and 7). On the other hand, of the three genes (NRAMP, EREB, and PP2B15) with heritability values less than 90%, the only gene that presented more than one eQTL associated with CLas multiplication was the EREB gene found in the two parental maps; the other two genes were only slightly enriched for eQTL (Tables 7 and 8). These results show that gene heritability is not a perfect predictor of eQTL detection. For gene expression values, as well as for other measurable variables, the power for detection of eQTL is largely but not exclusively determined by the gene's heritability value in a specific population (Visscher et al. 2008; Viñuela et al. 2012).

It was expected that a large number of eQTL would be found in the gene expression profiles for each candidate gene because we observed high heritability of the phenotypic characteristics and high saturation of the maps for each parent according to Curtolo et al. (2018); in addition, the population of hybrids selected for eQTL mapping consisted of 72 individuals. We found

Table 10 Relationship of genes that presented eQTL overlapped to QTL in regulatory networks for each linkage group (LG) in the two genetic maps constructed for each parent

LG	*C. sunki* map	*P. trifoliata* map
1	-	PP2B10 (84) and Starch (122)
3	GLUC (147), GALAC (173), PP2B10 (138) and Starch (127)	-
4	-	UDP (235), PAE (243), EREB (214) and CLas (258)
5	NAC2 (420) and CLas (412)	UDP (390), GLUC (440), EREB (343), PP2B15 (405), PP2B10 (386) and Starch (382)
6	GALAC (0), MEX1 (13), NRAMP (18) and PP2B10 (18) and CLas (13)	-
7	CARBOX (72), GLUC (82), BAM3 (49), EREB (102) and CLas (105)	CARBOX (142), PP2B10 (151) and CLas (137)
8b	-	CARBOX (40) and CLas (40)
9	-	PAE (224) and CLas (215)

In parentheses is the position from the beginning in cM

a higher number of eQTL per gene for *C. sunki* (six) than for *P. trifoliata* (four), consistent with the results of Lima et al. (2018). The UDP gene presented the highest number of eQTL (six) on the map of the *P. trifoliata* genitor, while in the *C. sunki* map, a greater number, seven eQTL, were found for the CARBOX gene. These two genes therefore present a greater number of chromosomal regions that affect their transcription levels in response to CLas infection in the two-parent maps. On the other hand, the genes that presented only one eQTL in the *P. trifoliata* map were GALAC, MEX1 and PP2B15, while in the *C. sunki* map the NRAMP gene displayed only one eQTL. Moreover, the NRAMP gene did not have eQTL in the *P. trifoliata* map, nor did the PAE gene in the *C. sunki* map. The NRAMP gene may not participate greatly in the defense response of hybrids against CLas infection.

In the present study, many eQTL are composed of loci with low effects (R^2 less than 10%), and a few are associated with marker regions with moderate effects (10 to 30%), equivalent to the R^2 values in other eQTL mapping studies (Anderson et al. 2007; Lima et al. 2018).

Studies of eQTL enable the identification of chromosomal regions that affect the expression of multiple genes; in these locations, so-called hotspots, many nearby, closely linked loci control the production of various gene transcripts. Such a phenomenon is indicated by the presence of a series of eQTL that overlap in the LGs of genetic maps, and it can be attributed to the presence of genome regions rich in intimately linked genes, identifying nearby eQTL, or to a single genomic region that regulates the transcription of a large number of genes, from the detection of distant eQTL (West et al. 2007; Lima et al. 2018). However, it has been reported in the literature that many hotspots control the expression of genes encoding enzymes involved in numerous metabolic pathways and that some hotspots may even regulate the pathway as a whole (Kirst et al. 2005; Rosa 2007; Lima et al. 2018).

Lima et al. (2018) used a strategy similar to that used in the present study to detect eQTL related to resistance to *P. parasitica* and also found a greater number of hotspots in the *C. sunki* map, in addition to detecting a higher mean number of hotspots per LG for the same parent. A large number of candidate genes were evaluated in this mapping study focusing on the *Phytophthora*-citrus pathosystem. The number of genes that had overlapping and localized eQTL in hotspots ranged from two to five on the genetic maps in our study (Table 9). Lima et al. (2018) identified two to eight genes in the genetic maps that had overlapping and localized eQTL in a single hotspot.

Comparing the eQTL obtained based on the relative expression data of the target genes and the QTL of the starch quantification in the inoculated group and CLas quantification (Ct values), it was expected that some eQTL would contribute to the phenotypes. This was evidenced by the finding of overlaps between eQTL and QTL, indicating the existence of complex regulatory networks for both gene expression and phenotype

(Sugiyama et al. 2014; Lima et al. 2018). It was observed that the positions in cM from the beginning of the overlapping eQTL/QTL were fairly close, with some exceptions showing a relatively large distance; QTL usually cover large regions of the genome (at least 20 cM) (Gion et al. 2000; Brown et al. 2003; Lima et al. 2018).

An overlap was observed between a CARBOX gene eQTL and a starch accumulation QTL (Table 10). The network is located exactly at marker 100035369|F|0 in LG 8b of the *P. trifoliata* map, approximately 40 cM from the beginning, indicating the presence of a complex network that actively regulates both gene expression and phenotype. The carboxylesterase (CARBOX) gene was studied in *Arabidopsis* infected with *Xanthomonas campestris* pv *vesicatoria*, and it was observed that CARBOX drastically affects the ability of the plant to control bacterial growth (Cunnac et al. 2007).

Some genes, such as the PP2B10 gene, had more than one phenotype-related eQTL. The PP2B10 presented two associated eQTL in the *C. sunki* map, one related to starch quantification in LG 3 and the other related to CLas quantification (Ct values) in LG 6. In the *P. trifoliata* map, the same gene had three phenotype-related eQTL, two related to starch quantification in LG 1 and LG 5 and one related to CLas quantification (Ct values) in LG 7. In transcriptome studies, this gene was found to be highly induced in HLB-susceptible citrus genotypes upon inoculation with CLas (Mafra et al. 2013; Zhong et al. 2015; Fu et al. 2016), whereas in the present study this gene was predominantly repressed; we observed its expression using the RT-qPCR technique in the segregating population of citrandarins. In addition to their involvement in vascular tissue differentiation, the phloem-protein (PP2) genes have several functions, including cell differentiation of sieved elements and host defense responses such as pore plugging of the screened element to prevent colonization by insects and pathogens, interaction with mesophyll plasmodesmata to increase the exclusion limit size, and control of cell-to-cell traffic (Dinant et al. 2003).

The co-localization of eQTL and QTL represents the association between the allelic state of genomic regions with the quantification of gene transcripts within QTL involved in the variation of phenotypic characteristics (Sugiyama et al. 2014; Lima et al. 2018). With the exception of the T6PP and BAC2 genes, all of the genes presented eQTL co-located with QTL, independent of the map and the phenotypic characteristics (CLas or starch quantification). This demonstrates that these genes are responsive to the pathogen and that they are related to CLas multiplication.

References

Albrecht U, Bowman KD (2012) Transcriptional response of susceptible and tolerant citrus to infection with Candidatus Liberibacter asiaticus. Plant Science 185–186:118–30

Amaral LIV, Gaspar M, Costa PMF, Aidar MPM, Buckeridge MS (2007) A new rapid and sensitive enzymatic method for extraction and quantification of starch in plant material. Hoehnea 34:425–431

Anderson JA, Chao S, Liu S (2007) Molecular breeding using a major QTL for Fusarium head blight resistance in wheat. Crop Science 47:112–119

Aritua V, Achor D, Gmitter FG, Albrigo G, Wang N (2013) Transcriptional and microscopic analyses of citrus stem and root responses to Candidatus Liberibacter asiaticus infection. PLoS One 8:e73742

Aryal K, McBride Z, Chen D, Xie J, Szymanski DB (2017) Analysis of protein complexes in Arabidopsis leaves using size exclusion chromatography and label-free protein correlation profiling. Journal of Proteomics 166:8–18

Asamizu E, Shimoda Y, Kouchi H, Tabata S, Sato S (2008) A positive regulatory role for LjERF1 in the nodulation process is revealed by systematic analysis of nodule-associated transcription factors of lotus japonicus. Plant Physiology 147:2030–2040

Asins MJ, Bernet GP, Ruiz C, Cambra M, Guerri J, Carbonell EA (2004) QTL analysis of citrus tristeza virus-citradia interaction. Theoretical and Applied Genetics 108:603–611

Boava LP, Sagawa CH, Cristofani-Yaly M, Machado MA (2015) Incidence of 'Candidatus Liberibacter asiaticus'-Infected Plants Among Citrandarins as Rootstock and Scion Under Field Conditions. Phytopathology 105:518–24

Boava LP, Cristofani-Yaly M, Machado MA (2017) Physiologic, Anatomic, and Gene Expression Changes in Citrus sunki, Poncirus trifoliata, and Their Hybrids After 'Candidatus Liberibacter asiaticus' Infection. Phytopathology 107:590–599

Boscariol-Camargo RL, Cristofani-Yaly M, Malosso A, Coletta-Filho HD, Machado MA (2010) Avaliação de diferentes genótipos de citros à infecção por Candidatus Liberibacter asiaticus, 31. Citrus Research & Technology, Cordeirópolis, pp 85–90

Bové JM (2006) Huanglongbing: a destructive, newly-emerging, century-old disease of citrus. Journal of Plant Pathology 88:7–37

Brown GR, Bassoni DL, Gill GP, Fontana JR, Wheeler NC, Megraw RA, Davis MF, Sewell MM, Tuskan GA, Neale DB (2003) Identification of quantitative trait loci influencing wood property traits in loblolly pine (Pinus taeda L.). III. QTL verification and candidate gene mapping. Genetics 164:1537–1546

Budahn H, Peterka H, Mousa MA, Ding Y, Zhang S, Li J (2009) Molecular mapping in oil radish (Raphanus sativus L.) and QTL analysis of resistance against beet cyst nematode (Heterodera schachtii). Theoretical and Applied Genetics 118:775–782

Burchell B, Nebert DW, Nelson DR, Bock KW, Iyanagi T, Jansen PL, Lancet D, Mulder GJ, Chowdhury JR, Siest G (1991) The UDP glucuronosyltransferase gene superfamily: suggested nomenclature based on evolutionary divergence. DNA and Cell Biology 10:487–494

Cellier M, Privé G, Belouchi A, Kwan T, Rodrigues V, Chia W, Gros P (1995) Nramp defines a family of membrane proteins. Proceedings of the National Academy of Sciences of the United States of America 92:10089–10093

Chang S, Puryear J, Cairney J (1993) A simple and efficient method for isolating RNA from pine trees. Plant Molecular Biology Reporter 11:113–116

Chen L, Storey JD (2006) Relaxed significance criteria for linkage analysis. Genetics 173:2371–2381

Churchill GA, Doerge RW (1994) Empirical threshold values for quantitative trait mapping. Genetics 138:963–971

Cunnac S, Wilson A, Nuwer J, Kirik A, Baranage G, Mudgett MB (2007) A conserved carboxylesterase is a suppressor of AVRBST-elicited resistance in Arabidopsis. Plant Cell 19:688–705

Curtolo M, Soratto TAT, Gazaffi R, Takita MA, Machado MA, Cristofani-Yaly M (2018) High-density linkage maps for Citrus sunki and Poncirus trifoliata using DArTseq markers. Tree Genetics Genomes 14:5

Dalio RJD, Magalhães DM, Rodrigues CM, Arena GD, Oliveira TS, Souza-Neto RS, Picchi SC, Martins PMM, Santos PJC, Maximo HJ, Pacheco IS, De Souza AA, Machado MA (2017) PAMPs, PRRs, effectors and R-genes associated with citrus-pathogen interactions. Annals of Botany 119:749–774

De Spiegelaere W, Dern-Wieloch J, Weigel R, Schumacher V, Schorle H, Nettersheim D, Bergmann M, Brehm R, Kliesch S, Vandekerckhove L, Fink C (2015) Reference gene validation for RT-qPCR, a note on different available software packages. PLoS One 10:1–13

Dinant S, Clark AM, Zhu Y, Vilaine F, Palauqui JC, Kusiak C, Thompson GA (2003) Diversity of the superfamily of phloem lectins (phloem protein 2) in angiosperms. Plant Physiology 131:114–28

Ernst HA, Olsen AN, Skriver K, Larsen S, Leggio LL (2004) Structure of the conserved domain of ANAC, a member of the NAC family of transcription factors. EMBO Reports 5:297–303

Etxeberria E, Gonzalez P, Achor D, Albrigo G (2009) Anatomical distribution of abnormally high levels of starch in HLB-affected Valencia orange trees. Physiological and Molecular Plant Pathology 74:76–83

Fan J, Chen C, Brlansky RH, Gmitter FGJ, Li ZG (2010) Changes in carbohydrate metabolism in Citrus sinensis infected with 'Candidatus Liberibacter asiaticus.' Plant Pathology 59:1037–1043

Fan J, Chen X, Achor DS, Brlansk RH, Li Z-G, Gmitter FG Jr (2013) Differential anatomical responses of tolerant and susceptible citrus species to the infection of "Candidatus Liberibacter asiaticus." Physiological and Molecular Plant Pathology 83:69–74

Ferro M, Salvi D, Brugière S, Miras S, Kowalski S, Louwagie M, Garin J, Joyard J, Rolland N (2003) Proteomics of the chloroplast envelope membranes from Arabidopsis thaliana. Molecular amp: Cellular Proteomics 2:325–345

Folimonova SY, Robertson CJ, Garnsey SM, Gowda S, Dawson WO (2009) Examination of the responses of different genotypes of citrus to huanglongbing (citrus greening) under different conditions. Phytopathology 99:1346–1354

Fu S, Shao J, Zhou C, Hartung JS (2016) Transcriptome analysis of sweet orange trees infected with 'Candidatus Liberibacter asiaticus' and two strains of Citrus Tristeza Virus. BMC Genomics 17:349

Fundecitrus. Available at: http://www.fundecitrus.com.br/. Accessed on July 30, 2017

Gantulga D, Turan Y, Bevan DR, Esen A (2008) The Arabidopsis At1g45130 and At3g52840 genes encode β-galactosidases with activity toward cell wall polysaccharides. Phytochemistry 69:1661–1670

Gazaffi R, Margarido G, Pastina MM, Mollinari M, Garcia A (2014) A model for quantitative trait loci mapping, linkage phase, and segregation pattern estimation for a full-sib progeny. Tree Genetics Genomes 10:791–801

Gion JM, Rech P, Grima-Pettenati J, Verhaegen D, Plomion C (2000) Mapping candidate genes in Eucalyptus with emphasis on lignification genes. Molecular Breeding 6:441–449

Grattapaglia D (2004) Integrating genomics into Eucalyptus breeding. Genetics and Molecular Research 3:369–379

Hall DG, George J, Lapointe SL (2015) Further investigations on colonization of Poncirus trifoliata by the Asian citrus psyllid - Science Direct. Crop Protection 72:112–118

Huang M, Roose ML, Yu Q, Du D, Yu Y, Zhang Y, Deng Z, Stover E, Gmitter FG (2018) Construction of high-density genetic maps and detection of QTLs associated with Huanglongbing tolerance in citrus. Frontiers in Plant Science 9:1694

Ishikawa K, Nakatani H, Katsuya Y, Fukazawa C (2007) Kinetic and structural analysis of enzyme sliding on a substrate: multiple attack in β-Amylase. Biochemistry 46:792–798

Jansen RC, Nap JP (2001) Genetical genomics: The added value from segregation. Trends in Genetics 17:388–391

Kim JS, Sagaram US, Burns JK, Li JL, Wang N (2009) Response of sweet orange (Citrus sinensis) to 'Candidatus Liberibacter asiaticus' infection: microscopy and microarray analyses. Phytopathology 99: 50–57

Kirst M, Basten CJ, Myburg AA, Zeng ZB, Sederoff RR (2005) Genetic architecture of transcript-level variation in differentiating xylem of a eucalyptus hybrid. Genetics 169:2295–2303

Koh EJ, Zhou L, Williams DS, Park J, Ding N, Duan YP, Kang BH (2012) Callose deposition in the phloem plasmodesmata and inhibition of phloem transport in citrus leaves infected with "Candidatus Liberibacter asiaticus". Protoplasma 249:687–697

Li W, Hartung JS, Levy L (2006) Quantitative real-time PCR for detection and identification of Candidatus Liberibacter species associated with citrus huanglongbing. Journal of Microbiological Methods 66: 104–115

Lima RPM, Curtolo M, Merfa MV, Cristofani-Yaly M, Machado MA (2018) QTL and eQTL mapping related to citrandarins' resistance to citrus gummosis disease. BMC Genomics 19:516

Livak KJ, Schmittgen TD (2001) Analysis of relative gene expression data using real-time quantitative PCR and. Methods 25:402–408

Lynch M, Walsh B (1998) Genetics and analysis of quantitative traits. Sinauer Associates, Sunderland

Machado MA, Locali-Fabris EC, Coletta-Filho HD (2010) Candidatus Liberibacter spp., agentes do huanglongbing dos citros. Citrus Research Technology 31:25–35

Mafra V, Kubo KS, Alves-Ferreira M, Ribeiro-Alves M, Stuart RM, Boava LP, Rodrigues CM, Machado MA (2012) Reference Genes for Accurate Transcript normalization in Citrus Genotypes under Different Experimental Conditions. PLoS one 7 (2):1–11

Mafra V, Martins PK, Francisco CS, Ribeiro-Alves M, Freitas-Astúa J, Machado MA (2013) Candidatus Liberibacter americanus induces significant reprogramming of the transcriptome of the susceptible citrus genotype. BMC Genomics 14:247

Marengo S (2009) Mapeamento genético de tangerina Sunki e Poncirus trifoliata para resistência ao Huanglongbing (greening) dos citros. 75p. Online: http://www.dominiopublico.gov.br/pesquisa/DetalheObraForm.do?select_action=&co_obra=146568

Margarido GRA, Souza AP, Garcia AAF (2007) OneMap software for genetic mapping in outcrossing species. Hereditas 144:78–79

McLennan AG (2006) The Nudix hydrolase superfamily. Cellular and Molecular Life Sciences 63:123

Morgan JK, Shatters RG, Stover E, Duan YP, Moore GA, Powell CA, Jarra-Cavieres A, Clark S (2014) Clues into the metagenome of Huanglongbing infected Citrus by analysis of ancillary sequences from Ion Torrent whole genome Candidatus Liberibacter asiaticus sequencing. Journal of Citrus Pathology, 1. https://escholarship.org/uc/item/4b22q45m

Murray MG, Thompson WF (1980) Rapid isolation of high molecular weight plant DNA. Nucleic Acids Research 8:4321–4325

Philippe F, Pelloux J, Rayon C (2017) Plant pectin acetylesterase structure and function: new insights from bioinformatic analysis. BMC Genomics 18:456

Porto BN, Magalhaes PC, Campos NA, Alves JD, Magalhães MM (2010) Otimização de protocolos de extração de RNA em diferentes tecidos de milho. Revista Brasileira de Milho e Sorgo 9:189–200

Raiol-Junior LL, Baia ADB, Luiz FQBF, Fassini CG, Marques VV, Lopes SA (2017) Improvement in the Excised Citrus Leaf Assay to Investigate Inoculation of 'Candidatus Liberibacter asiaticus' by the Asian Citrus Psyllid Diaphorina citri. Plant Disease 101:409–413

Rebai A (1997) Comparison of methods for regression interval mapping inQTL analysis with non-normal traits. Genetics Research 69:69–74

Richardson ML, Hall DG (2014) Resistance of Poncirus and Citrus x Poncirus Germplasm to the Asian Citrus Psyllid. Journal of Citrus Pathology 1. https://escholarship.org/uc/item/73z3s5hx

Rigano LA, Malamud F, Orce IG, Filippone MP, Marano MR, Amaral AMd, Castagnaro AP, Vojnov AA (2014) Rapid and sensitive detection of Candidatus Liberibacter asiaticus by loop mediated isothermal amplification combined with a lateral flow dipstick. BMC Microbiology 14:86

Rosa GJDM (2007) Delineamento de experimentos em genética genômica. Revista Brasileira de Zootecnia 36:211–218

Saurin W, Hofnung M, Dassa E (1999) Getting in or out: early segregation between importers and exporters in the evolution of ATP-Binding Cassette (ABC) transporters. Journal of Molecular Evolution 48:22–41

Shi C, Uzarowska A, Ouzunova M, Landbeck M, Wenzel G, Lübberstedt T (2007) Identification of candidate genes associated with cell wall digestibility and eQTL (expression quantitative trait loci) analysis in a Flint × Flint maize recombinant inbred line population. BMC Genomics 8:22

Sugiyama A, Omura M, Shimada T, Fujii H, Endo T, Shimizu T, Nesumi H, Nonaka K, Ikoma Y (2014) Expression quantitative trait loci analysis of carotenoid metabolism-related genes in citrus. Journal of the Japanese Society for Horticultural Science 83:32–43

Teixeira DC, Saillard C, Couture C, Martins EC, Wulff NA, Eveillard-Jagoueix S, Yamamoto PT, Ayres AJ, Bove JM (2008) Distribution and quantification of Candidatus Liberibacter americanus, agent of huanglongbing disease of citrus in Sao Paulo State, Brasil, in leaves of an affected sweet orange tree as determined by PCR. Molecular and Cellular Probes 22:139–150

Viñuela A, Snoek LB, Riksen JAG, Kammenga JE (2012) Aging Uncouples Heritability and Expression-QTL in Caenorhabditis elegans. G3: Genes, Genomes, Genetics 2:597–605

Visscher PM, Hill WG, Wray NR (2008) Heritability in the genomics era - concepts and misconceptions. Nature Reviews Genetics 9:255–266

Wang Z, Yin Y, Hu H, Yuan Q, Peng G, Xia Y (2006) Development and application of molecular based diagnosis for 'Candidatus Liberibacter asiaticus', the causal pathogen of citrus huanglongbing. Plant Pathology 55:630–638

Wang N, Trivedi P (2013) Citrus Huanglongbing: A newly relevant disease presents unprecedented challenges. Phytopathology 103(7): 652–65

Wang Y, Han Y, Teng W, Zhao X, Li Y, Wu L, Li D, Li W (2014) Expression quantitative trait loci infer the regulation of isoflavone accumulation in soybean (Glycine max L. Merr.) seed. BMC Genomics 15:680

Wang Y, Zhou L, Yu X, Stover E, Luo F, Duan Y (2016) Transcriptome profiling of Huanglongbing tolerant and susceptible citrus plants reveals the role of basal resistance in HLB tolerance. Frontiers in Plant Science 7:933

Wang N, Pierson EA, Setubal JC, Xu J, Levy JG, Zhang Y, Li J, Rangel LT Jr (2017) The Candidatus liberibacter–host interface: Insights into pathogenesis mechanisms and disease control. Annual Review of Phytopathology 55:451–482

West MA, Kim K, Kliebenstein DJ, van Leeuwen H, Michelmore RW, Doerge RW, St Clair DA (2007) Global eQTL mapping reveals the complex genetic architecture of transcript-level variation in *Arabidopsis*. Genetics 175:1441–1450

Yan AO, Zhi-qiu HU, Zai-xiang TANG, Xue-feng WANG, Chen-wu XU (2009) General method for QTL mapping in multiple related populations derived from multiple parents. Rice Science 16:45–50

Young ND (1994) Construction a plant genetic linkage map with DNA markers. In: Philips PL, Vasil IK (eds) DNA-based markers in plants. Kluwer Academic Publisher, Dordrecht, pp 39–57

Zeng ZB (1993) Theoretical basis for separation of multiple linked gene effects in mapping quantitative trait loci. Proceedings of the National Academy of Sciences of the United States of America 90:10972–6

Zhang Y, Zagnitko O, Rodionova I, Osterman A, Godzik A (2011) The FGGY Carbohydrate Kinase Family: Insights into the evolution of functional specificities. PLoS Computational Biology 7:e1002318

Zhao S, Fernald RD (2005) Comprehensive algorithm for quantitative real-time polymerase chain reaction. Journal of Computational Biology 12:1047–1064

Zhong Y, Cheng C, Jiang N, Jiang B, Zhang Y, Wu B et al (2015) Comparative transcriptome and iTRAQ proteome analyses of citrus root responses to *Candidatus* Liberibacter asiaticus infection. PLoS One 10:e0126973